BENNETT

AI-POWERED BIOLOGICAL INTELLIGENCE

IDENTIFYN RESOLUTION STEPDOWN

ATM.P

MICROSCOPY EVIDENCE ASSESSMENT

Rabbit anti-Human ATM.p (Serine 1981) Recombinant Monoclonal - Identifyn® SRM Alexa Fluor™ 647

WESTERN BLOT -> WIDEFIELD -> CONFOCAL -> AIRYSCAN -> SINGLE-MOLECULE STORM

5	0	PENDING
ORDERED EVIDENCE TIERS	SUPPORTING CONTROL	SCIENTIST REVIEW

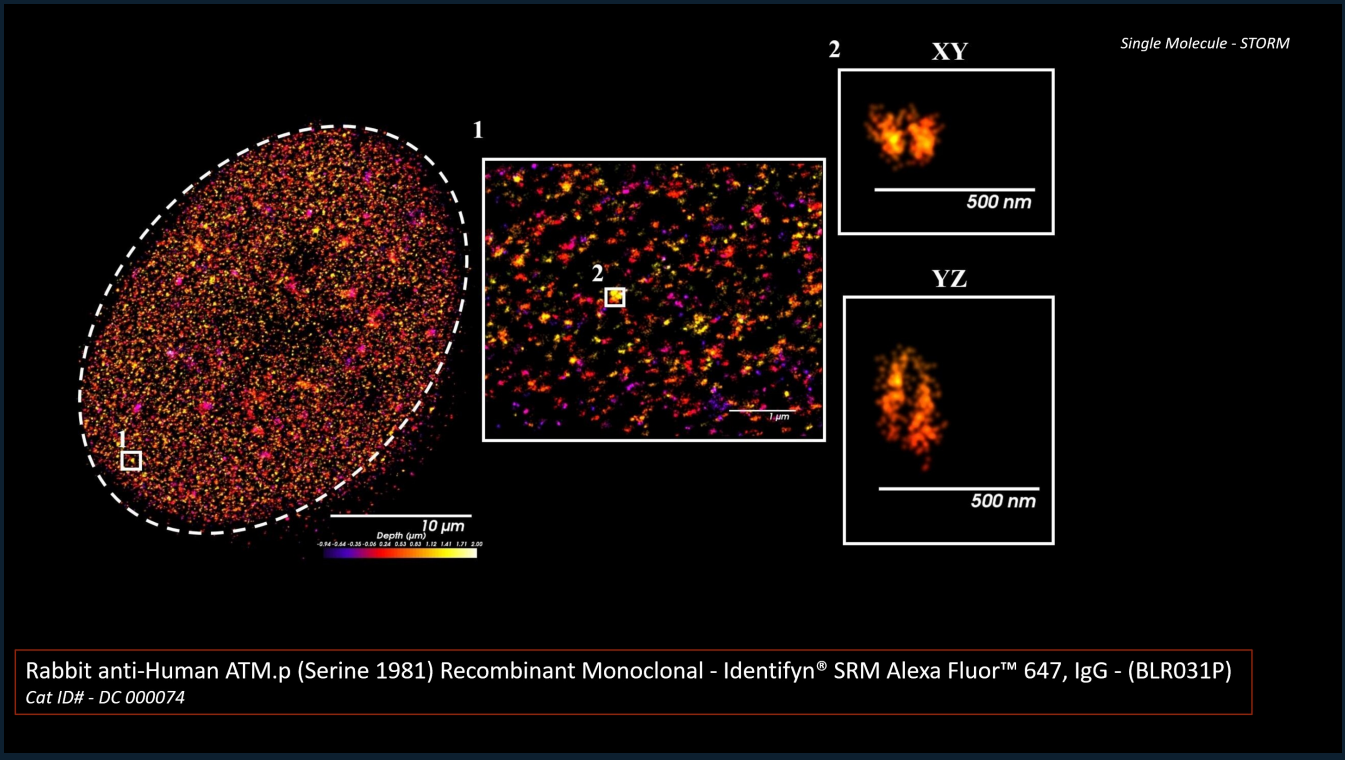

Rabbit anti-Human ATM.p (Serine 1981) Recombinant Monoclonal - Identifyn® SRM Alexa Fluor™ 647, IgG - (BLR031P)
Cat ID# - DC 000074

REPRESENTATIVE HIGHEST-AVAILABLE VIEW / SINGLE-MOLECULE STORM

DC-000074 | PRODUCT-LEVEL EVIDENCE DOSSIER

SOURCE-GROUNDED MICROSCOPY + BIOLOGICAL REVIEW / IDENTIFYN EVIDENCE PRESERVED

CRO CAPABILITY DEMONSTRATED

Identifyn performed the experimental and imaging work documented below. BENNETT converts that operating history into a governed, source-bounded scientific record.

- Source-documented sample preparation and antibody/reagent workflow
- Western blot imaging
- Widefield fluorescence microscopy
- Confocal microscopy
- Airyscan acquisition and reconstruction workflow
- Single-molecule STORM presentation workflow
- Treatment-response experimental workflow
- Z-stack / 3D acquisition
- Multi-channel imaging

SCIENTIFIC QUESTION

What source-bounded experimental and microscopy evidence is preserved for ATM.p, and what is the strongest interpretation allowed by the available modalities and controls?

EVIDENCE AVAILABLE

Western blot -> Widefield -> Confocal -> Airyscan -> Single-molecule STORM

BENNETT ASSESSMENT

The preserved DC-000074 record contains Western blot; Widefield; Confocal; Airyscan; Single-molecule STORM. Missing modalities are not represented or inferred.

BENNETT / MICROSCOPY AND BIOLOGICAL EVIDENCE REVIEW

SOURCE-GROUNDED RETROSPECTIVE REVIEW / PENDING SCIENTIST REVIEW

SOURCE STATE	SOURCE HASH VERIFIED / EVENT RECORDED
BENNETT EVIDENCE REVIEW	COMPLETED / SOURCE-BOUNDED
NATIVE IMAGE REPROCESSING	NOT PERFORMED
LITERATURE SOURCES	INDEPENDENTLY VERIFIED
SCIENTIST REVIEW	PENDING
PUBLICATION	NOT AUTHORIZED

OVERALL CALL / PARTIAL STEPDOWN / SOURCE-BOUNDED REVIEW

The preserved DC-000074 record contains Western blot; Widefield; Confocal; Airyscan; Single-molecule STORM. Missing modalities are not represented or inferred.

SETTINGS ASSESSMENT

The record preserves 5 ordered evidence tier(s). Structured source metadata values are reported by stage and remain tied to the original method objects.

BIOLOGICAL SUPPORT

The record supports retrospective, source-bounded microscopy review. Target identity, specificity, treatment effect, binding, interaction and mechanism are not inferred from presentation images alone.

CONTROL ASSESSMENT

No separate control record is preserved; none is inferred from method or template language.

CLAIM CEILING

This draft supports historical capability documentation, source registration, modality ordering, settings review and bounded interpretation. It does not independently validate antibody specificity, quantify a population response, establish binding, interaction, causation or mechanism, or authorize publication.

PROCESSING DISCLOSURE

Retrospective BENNETT architectural evaluation of preserved Identifyn source evidence. BENNETT did not perform native-file reprocessing, new deterministic measurement or the historical image post-processing represented in this record.

REAGENTS AND ACQUIRED CHANNELS

Preparation reagents are reported separately from channels actually documented in the acquisition settings. Fluorophores mentioned in staining are not automatically treated as acquired channels.

EVIDENCE OBJECT	REAGENTS / FLUOROPHORES PRESENT	CHANNELS ACTUALLY ACQUIRED
Western blot	647	Not deterministically stated in the acquisition block
Widefield	405/DAPI; 647	2; 50 Cy 5; 49 DAPI; 625 - 655; 335 - 383; 665 - 715; 420 - 470; 653
Confocal	405/DAPI; 488; 647	2; None; 639 nm @ 2.00%; 405 nm @ 0.8%; 653; 353; 668; 465
Airyscan	405/DAPI; 488; 647	3; None; 639 nm @ 1.10%; 405 nm @ 1.0%; 653; 353; 668; 465
Single-molecule STORM	647	Both Channels

MODALITY ASSESSMENT / PART 1 OF 5

Western blot / SOURCE EVIDENCE PRESERVED

DOCUMENTED SETTINGS

Platform: Azure Sapphire FL. Objective: not explicitly stated. Platform: Azure Sapphire FL with Customizable Laser and Filter Modules, Enabling UV-NIR and Z-Plane Imaging.. Structured source metadata values: 11.

VISIBLE OBSERVATION

A preserved presentation image is available for Western blot. BENNETT records the visible source presentation without creating a new native measurement.

SOURCE-REPORTED RESULT

The source identifies this object as Western blot, documents platform context as Azure Sapphire FL, and records detected dye/channel descriptors as 647.

LITERATURE CORRELATION

Consistent with peer-reviewed microscopy and antibody-validation guidance that presentation evidence must remain bounded by modality, controls and source documentation.

INTERPRETIVE LIMIT

Band position and displayed intensity do not independently establish analytical specificity, target identity, linearity, or treatment effect.

CLAIM CEILING

This tier supports a source-bounded statement that the historical Western blot evidence and documented settings are preserved for review; stronger biological or quantitative conclusions require compatible native data, controls and scientist review.

MODALITY ASSESSMENT / PART 2 OF 5

Widefield / SOURCE EVIDENCE PRESERVED

DOCUMENTED SETTINGS

Platform: ZEISS Axio Imager.M1. Objective: Plan-Apochromat 63x/1.40 Oil M27. Platform: Zeiss Axio Imager.M1 Widefield, using a Plan-Apochromat 63x/1.40 Oil M27, Axiocam 705, and X-Cite Xylis Lamp, was used with the following parameters for each dye:. Acquisition: Channels: 2; Scaling (Per Pixel): 0.110 µm X 0.110 µm; Image size (Pixels): 711 X 636; Image Size (Pixels): 711 X 636; Bit Depth: 14 Bit. Detector/camera: Imaging Device: Axiocam 705. Timing: Exposure Time: 250 ms; 25 ms. Illumination: Light source: X-Cite Xylis Lamp Intensity @ 25.00%; X-Cite Xylis Lamp Intensity @ 10.00%. Optical/scan: Effective NA: 1.4. Structured source metadata values: 39.

VISIBLE OBSERVATION

A preserved presentation image is available for Widefield. BENNETT records the visible source presentation without creating a new native measurement.

SOURCE-REPORTED RESULT

The source identifies this object as Widefield, documents platform context as ZEISS Axio Imager.M1, and records detected dye/channel descriptors as 405/DAPI; 647.

LITERATURE CORRELATION

Consistent with peer-reviewed microscopy and antibody-validation guidance that presentation evidence must remain bounded by modality, controls and source documentation.

INTERPRETIVE LIMIT

A presentation image supports gross localization and source-bounded co-occurrence, not direct binding, molecular colocalization, or native quantitative measurement.

CLAIM CEILING

This tier supports a source-bounded statement that the historical Widefield evidence and documented settings are preserved for review; stronger biological or quantitative conclusions require compatible native data, controls and scientist review.

MODALITY ASSESSMENT / PART 3 OF 5

Confocal / SOURCE EVIDENCE PRESERVED

DOCUMENTED SETTINGS

Platform: ZEISS LSM 980. Objective: Plan-Apochromat 63x/1.40 Oil DIC M27. Platform: Zeiss LSM 980 Confocal with NIR Detection, Axio Observer.Z1/7, using a Plan-Apochromat 63x/1.40 Oil DIC M27, was used with the following parameters for each dye:. Acquisition: Z-Stack: 151 Slices (4.5 µm); Channels: 2; Scaling (Per Pixel): 0.059 µm X 0.059 µm X 0.030 µm; Image size (Pixels): 1406 X 1041; Image Size (Pixels): 1406 X 1041; Bit Depth: 16 Bit. Detector/camera: Imaging Device: GaAsP-Pmt3; Detector Type: GaAsP-PMT. Timing: Pixel Time: 0.26 µs; Frame Time: 5.63 s. Illumination: Laser Wavelength: 639 nm @ 2.00%; 405 nm @ 0.8%. Optical/scan: Pinhole: 1.00 AU / 66 µm; 1.00 AU / 44 µm; Scan Zoom: 1.5; LSM Scan Speed: 11; Scan Direction: Bidirectional; Averaging: 8; Effective NA: 1.4. Processing: LSM Plus Mode: Filter: 7.8 (3D, Auto); Filter: 6.8 (3D, Auto). Structured source metadata values: 44.

VISIBLE OBSERVATION

A preserved presentation image is available for Confocal. BENNETT records the visible source presentation without creating a new native measurement.

SOURCE-REPORTED RESULT

The source identifies this object as Confocal, documents platform context as ZEISS LSM 980, and records detected dye/channel descriptors as 405/DAPI; 488; 647.

LITERATURE CORRELATION

Consistent with peer-reviewed microscopy and antibody-validation guidance that presentation evidence must remain bounded by modality, controls and source documentation.

INTERPRETIVE LIMIT

Optical sectioning and source-bounded 3D presentation do not establish binding, mechanism, or population-level effect.

CLAIM CEILING

This tier supports a source-bounded statement that the historical Confocal evidence and documented settings are preserved for review; stronger biological or quantitative conclusions require compatible native data, controls and scientist review.

MODALITY ASSESSMENT / PART 4 OF 5

Airyscan / SOURCE EVIDENCE PRESERVED

DOCUMENTED SETTINGS

Platform: ZEISS LSM 980. Objective: Plan-Apochromat 63x/1.40 Oil DIC M27. Platform: Zeiss LSM 980 Confocal with NIR Detection, Axio Observer.Z1/7, using a Plan-Apochromat 63x/1.40 Oil DIC M27, was used with the following parameters for each dye:. Acquisition: Z-Stack: 161 Slices (4.8 µm); Channels: 3; Scaling (Per Pixel): 35.30 nm X 35.30 nm X 30.00 nm; Image size (Pixels): 1045 X 937; Image Size (Pixels): 1045 X 937; Bit Depth: 16 Bit. Detector/camera: Imaging Device: Airyscan; Detector Type: GaAsP-PMT. Timing: Pixel Time: 1.10 µs; Frame Time: 18.77 s. Illumination: Laser Wavelength: 639 nm @ 1.10%; 405 nm @ 1.0%. Optical/scan: Pinhole: 5.00 AU / 328 µm; 5.00 AU / 215 µm; Scan Zoom: 2.0; LSM Scan Speed: 6; Scan Direction: Bidirectional; Averaging: 4; Effective NA: 1.4. Processing: Projection: View Angle 35°, Scale Z 100%, Reverse Z-Axis NOT Selected, Stereo Anaglyph NOT Selected, Camera Separation 5% (deselected), Parallax Shift 0% (deselected); Background: Black; AiryScan Mode: Super Resolution: 10.0 (3D, Auto); Super Resolution: 8.9 (3D, Auto). Structured source metadata values: 57.

VISIBLE OBSERVATION

A preserved presentation image is available for Airyscan. BENNETT records the visible source presentation without creating a new native measurement.

SOURCE-REPORTED RESULT

The source identifies this object as Airyscan, documents platform context as ZEISS LSM 980, and records detected dye/channel descriptors as 405/DAPI; 488; 647.

LITERATURE CORRELATION

Consistent with peer-reviewed microscopy guidance that advanced-resolution outputs remain dependent on acquisition, reconstruction or localization quality control.

INTERPRETIVE LIMIT

Displayed feature separation remains reconstruction dependent; no unsupported numerical resolution or molecular architecture claim is permitted.

CLAIM CEILING

This tier supports a source-bounded statement that the historical Airyscan evidence and documented settings are preserved for review; stronger biological or quantitative conclusions require compatible native data, controls and scientist review.

MODALITY ASSESSMENT / PART 5 OF 5

Single-molecule STORM / SOURCE EVIDENCE PRESERVED

DOCUMENTED SETTINGS

Platform: Bruker Vutara VXL. Objective: Olympus 60x/1.30 Silicon Oil Objective. Platform: Bruker Vutara VXL Biplane Single Molecule Microscope, using an Olympus 60x/1.30 Silicon Oil Objective, was used with the following parameters:. Detector/camera: Camera: Both Cameras. Timing: Exposure Time: 20 ms Selected; Super Resolution Camera Exposure Time: 20 ms; Widefield Camera Exposure Time: 100 ms. Illumination: Photoactivation/Imaging Laser: 0% Selected. Structured source metadata values: 79.

VISIBLE OBSERVATION

A preserved presentation image is available for Single-molecule STORM. BENNETT records the visible source presentation without creating a new native measurement.

SOURCE-REPORTED RESULT

The source identifies this object as Single-molecule STORM, documents platform context as Bruker Vutara VXL, and records detected dye/channel descriptors as 647.

LITERATURE CORRELATION

Consistent with peer-reviewed microscopy guidance that advanced-resolution outputs remain dependent on acquisition, reconstruction or localization quality control.

INTERPRETIVE LIMIT

Without localization tables, uncertainty, blinking, drift, and independent cluster evidence, the presentation cannot establish molecule count, cluster truth, exact precision, or molecular architecture.

CLAIM CEILING

This tier supports a source-bounded statement that the historical Single-molecule STORM evidence and documented settings are preserved for review; stronger biological or quantitative conclusions require compatible native data, controls and scientist review.

CROSS-MODALITY SYNTHESIS

The preserved DC-000074 record contains Western blot; Widefield; Confocal; Airyscan; Single-molecule STORM. Missing modalities are not represented or inferred.

Different acquisitions are not treated as a quantitative intensity ladder. Any continuity statement remains qualitative and source bounded.

BENNETT LITERATURE CORRELATION — SOURCES INDEPENDENTLY VERIFIED

BENNETT uses independently verified primary scientific sources to test whether the interpretation is scientifically consistent and properly bounded. Literature correlation does not retroactively validate the Identifyn dataset or replace scientist review.

- Antibody and microscopy evidence require orthogonal controls and modality-appropriate interpretation; presentation images alone do not establish analytical specificity.

- Advanced-resolution presentation depends on acquisition, reconstruction or localization quality control before numerical resolution, molecular dimensions or cluster identity can be claimed.

REFERENCES

1. Uhlen M, et al. A proposal for validation of antibodies. Nat Methods. 2016;13:823-827. doi:10.1038/nmeth.3995.
2. Gustafsson MGL. Surpassing the lateral resolution limit by a factor of two using structured illumination microscopy. J Microsc. 2000;198:82-87. doi:10.1046/j.1365-2818.2000.00710.x.
3. Sage D, et al. Quantitative evaluation of software packages for single-molecule localization microscopy. Nat Methods. 2015;12:717-724. doi:10.1038/nmeth.3442.

RELEASE BOUNDARY

This assessment remains a draft pending scientist review. No publication is authorized. Any future native-file analysis must enter BENNETT as a new evidence snapshot with routed engine authority, native-data QA, methods, limitations, and an independently reviewed claim ceiling.

SOURCE RECONCILIATION / QA / PROVENANCE

SOURCE STATUS - PRESERVED / AUTO-RECONCILED

Historical Identifyn source material was subjected to BENNETT retrospective QA. Original source state and correction history remain preserved in provenance.

HIGH CONFIDENCE - AUTO-RECONCILED

Airyscan / Scaling (Per Pixel): 35.30 nm X 35.30 nm X 30.00 nm -> 0.03530 µm X 0.03530 µm X 0.03000 µm. Both numerical magnitude and unit were normalized, then checked against the reported field dimensions; no unit label was changed alone. Supporting evidence: Image Size (Pixels)=1045 X 937; Image Size (Scaled)=36.88 µm X 33.07 µm; PASS - INTERNALLY CONSISTENT. Documented sampling reproduces the reported physical field dimensions. Maximum field-dimension error 0.02%.

HIGH CONFIDENCE - SOURCE-DERIVED METADATA CANONICALIZATION

Product identity / phosphosite: Blank structured canonical field -> Serine 1981. The phosphorylation site is explicitly stated in the preserved source product identity. Supporting evidence: Rabbit anti-Human ATM.p (Serine 1981) Recombinant Monoclonal - Identifyn® SRM Alexa Fluor™ 647

BENNETT

AI-POWERED BIOLOGICAL INTELLIGENCE

BENNETT EVIDENCE REVIEW COMPLETE

INTERPRETATION TO EVIDENCE

BENNETT has completed the bounded retrospective assessment.
The following pages switch ownership to the preserved Identifyn record.

IDENTiFYN®

IDENTIFYN PRESERVED SOURCE EVIDENCE

ORIGINAL RECORD BEGINS

Images, source methods, acquisition settings and provenance follow in the locked Stepdown order. Scientific wording is preserved; missing modalities are not invented. No separate control record is present in the preserved product record.

PRODUCT-LEVEL STEPDOWN MAP

This dossier preserves the complete available evidence progression for DC-000074. Each tier remains tied to its original image, source method, instrument context and cryptographic identity. No separate control record is present in the preserved product record, and none is inferred.

CANONICAL STEPDOWN TIER	EVIDENCE STAGE	INSTRUMENT	STATUS
1	Western blot	Azure Sapphire FL	PRESERVED
2	Widefield	ZEISS Axio Imager.M1	PRESERVED
4	Confocal	ZEISS LSM 980	PRESERVED
5	Airyscan	ZEISS LSM 980	PRESERVED
8	Single-molecule STORM	Bruker Vutara VXL	PRESERVED

INTERPRETIVE BOUNDARY

Ordering evidence by resolution tier does not make the modalities interchangeable. Each stage retains its acquisition environment and scientific limitations. This pilot organizes the record; it does not synthesize new biological claims.

ORIGINAL IMAGE EVIDENCE / WESTERN BLOT

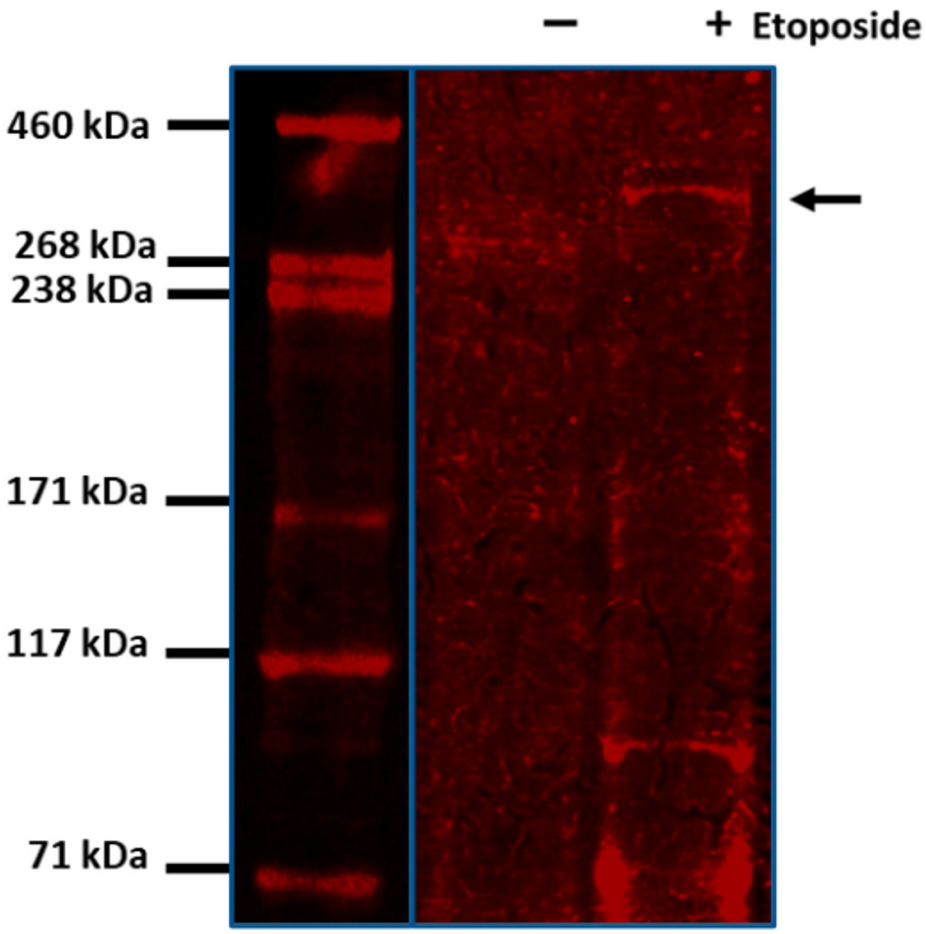

EVIDENCE TIER	Western blot
INSTRUMENT	Azure Sapphire FL
CELL MODEL	HeLa
DETECTED DYES	647
METADATA VALUES	11

STRUCTURED ACQUISITION METADATA / WESTERN BLOT

The values below were deterministically extracted from the preserved Identifyn method PDF text. They remain source-documented metadata, not new BENNETT measurements.

FIELD	SOURCE-DOCUMENTED VALUE
Platform / configuration	Azure Sapphire FL with Customizable Laser and Filter Modules, Enabling UV-NIR and Z-Plane Imaging.
Scanner	Azure Sapphire FL with Customizable Laser and Filter Modules, Enabling UV-NIR and Z-Plane Imaging.
Detection mode	Fluorescence
Laser	638 nm
Emission Filter	676 ± 37 nm
Detector	PMT
Intensity	L3
Pixel size	100 µm
Scan Speed	High
Quality	High
Focus	Membrane (0 µm in Z-axis)
Image	S. Khanal

SOURCE METHOD

The text below is carried from the preserved Identifyn source record. Typography and pagination have been normalized for this preservation dossier; scientific wording has not been editorially rewritten.

Identifyn Standards for Optical Microscopy Methods™

Identifyn® Primary Antibody

Rabbit anti-Human ATM.p (Serine 1981) Recombinant Monoclonal - Identifyn® SRM Alexa Fluor™ 647, IgG - (BLR031P)
Cat ID# - DC 000074

Expected MW: 350 kDa

HeLa cells were treated with 2 µM etoposide for 12 hours to induce DNA damage. Cells were homogenized using an ultrasonication probe and a nuclear lysis buffer, then centrifuged to pellet the cell debris. The lysate supernatant (100 µg) was mixed with NuPAGE™ LDS Sample Buffer (4X), heated at 80 °C for 10 min, and subjected to electrophoresis on NuPAGE™ Tris-Acetate Mini Protein Gels (3-8%, 1.0 mm) in a Mini Gel Tank. Thermo Fisher's HiMark™ Pre-stained Protein Standard was used as a molecular weight marker.

Post-electrophoresis, the proteins were transferred to a polyvinylidene difluoride (PVDF) membrane using the iBlot™ 3 Starter Kit PVDF. The transfer membrane was blocked with Blocker™ Casein for 1 hour, then washed 5 times with 1X PBS. The blocked membrane was incubated with Rabbit anti-Human ATM.p (Serine 1981) Recombinant Monoclonal - Identifyn® SRM Alexa Fluor™ 647 IgG - (BLR031P) for 20 hours, followed by five washes in 1X PBS. The membrane was dried for 10 minutes at room temperature before imaging.

Scanner = Azure Sapphire FL with Customizable Laser and Filter Modules, Enabling UV-NIR and Z-Plane Imaging.

Scan Settings

Detection mode = Fluorescence
Laser = 638 nm
Emission Filter = 676 ± 37 nm
Detector = PMT
Intensity = L3
Pixel size = 100 µm
Scan Speed = High
Quality = High
Focus = Membrane (0 µm in Z-axis)

Post Processing

NONE

Image: S. Khanal

SOURCE PROVENANCE

Catalog	DC-000074
Stage	Western blot
Instrument	Azure Sapphire FL
Microscope configuration	Azure Sapphire FL with Customizable Laser and Filter Modules, Enabling UV-NIR and Z-Plane Imaging.
Structured source metadata values	11
Metadata source	PRESERVED_SOURCE_METHOD_PDF_TEXT
Cell model	HeLa
Image SHA-256	DDB088CE3C5EE9311FB2B6123E23629DB96E2D1FFD0CD54F37E9E96BED4E0400
Method PDF SHA-256	CC0CE75E0C8315C53D839741ECACD95434A0471BBB706C99CE65630060CB4FB6

ORIGINAL IMAGE EVIDENCE / WIDEFIELD

Panel A depicts widefield fluorescence microscopy of the Rabbit anti-Human ATM.p (Serine 1981) Recombinant Monoclonal - Identifyn® SRM Alexa Fluor™ 647, IgG – (BLR031P) following DNA damage induction. The left panel shows direct ATM.p signal localization; the middle panel displays DAPI nuclear counterstaining; and the right panel shows the merged image. Strong nuclear-associated fluorescence and discrete foci formation were observed, demonstrating effective target localization and preservation of signal integrity following direct conjugation. These observations are consistent with the corresponding unconjugated stepdown dataset generated using Rabbit anti-Human ATM.p (Serine 1981) Recombinant Monoclonal, IgG (BLR031P) (Cat ID# - PA-RR 000012), supporting equivalent staining behavior and confirming robust fluorophore conjugation.

Panel B shows the Zeiss ZEN acquisition interface and associated imaging parameters utilized during image collection. Widefield excitation was performed using the X-Cite Xylis LED illumination system operating at 25% lamp power, while image acquisition was performed on the Zeiss Axiocam 705 camera using an exposure time of 250 ms. These acquisition settings closely mirrored those required for the unconjugated primary antibody workflow, further supporting preservation of signal strength and fluorophore efficiency following direct conjugation to Identifyn® SRM Alexa Fluor™ 647.

Panel C presents a 2.5D fluorescence intensity representation generated from the acquired widefield dataset. Intensity mapping demonstrated strong nuclear localization and pronounced Phospho- ATM foci formation in association with DAPI-positive nuclei. Quantitative analysis performed with the Zeiss ZEN histogram tool showed a maximum fluorescence intensity of 5,188.00, further supporting the robustness of the conjugation under standard widefield LED excitation and collection parameters. Collectively, these findings demonstrate that the direct conjugate maintains robust signal generation, nuclear specificity, and compatibility with conventional widefield fluorescence microscopy workflows.

EVIDENCE TIER	Widefield
INSTRUMENT	ZEISS Axio Imager.M1
CELL MODEL	HeLa
DETECTED DYES	405/DAPI; 647
METADATA VALUES	39

STRUCTURED ACQUISITION METADATA / WIDEFIELD

The values below were deterministically extracted from the preserved Identifyn method PDF text. They remain source-documented metadata, not new BENNETT measurements.

FIELD	SOURCE-DOCUMENTED VALUE
Platform / configuration	Zeiss Axio Imager.M1 Widefield, using a Plan-Apochromat 63x/1.40 Oil M27, Axiocam 705, and X-Cite Xylis Lamp, was used with the following parameters for each dye:
Objective	Plan-Apochromat 63x/1.40 Oil M27
Channels	2
Scaling (Per Pixel)	0.110 µm X 0.110 µm
Image Size (Pixels)	711 X 636
Image Size (Scaled)	77.87 µm X 69.66 µm
Bit Depth	14 Bit
Image Center Position	X: 0.00 µm, Y: 0.00 µm
ROI Center Offset	X: 0.00 µm, Y: 0.00 µm
Reflector	50 Cy 5 | 49 DAPI
Beam Splitter	660 | 395
Filter Excitation Wavelength	625 - 655 | 335 - 383
Filter Emission Wavelength	665 - 715 | 420 - 470
Contrast Method	Fluorescence
Light Source	X-Cite Xylis Lamp Intensity @ 25.00% | X-Cite Xylis Lamp Intensity @ 10.00%
Exposure Time	250 ms | 25 ms
Excitation Wavelength	653 | 353
Emission Wavelength	668 | 465
Effective NA	1.4
Imaging Device	Axiocam 705
Camera Adapter	1x Camera Adapter
Depth of Focus	1.03 µm | 0.72 µm
Binning Mode	2,2
Render Mode	Surface
Grid distance	5
Angle X	54
Angle Y	-180
Z Scaling	1.0
Ambient	50
Specular	20
Shininess	50
Light Height	2.0

SOURCE METHOD

The text below is carried from the preserved Identifyn source record. Typography and pagination have been normalized for this preservation dossier; scientific wording has not been editorially rewritten.

Identifyn Standards for Optical Microscopy Methods™

Identifyn® Primary Antibody

Rabbit anti-Human ATM.p (Serine 1981) Recombinant Monoclonal - Identifyn® SRM Alexa Fluor™ 647, IgG - (BLR031P)
Cat ID# - DC 000074

ATM (ataxia-telangiectasia mutated) is a crucial serine/threonine kinase that plays a central role in the DNA damage response (DDR), particularly in response to DNA double-strand breaks (DSBs). ATM's activation and subsequent phosphorylation cascades are essential for detecting DNA damage and initiating repair processes. Here's a detailed overview of how ATM is activated, its targets, and its role in the DDR:

Activation of ATM
In response to DNA damage, particularly DSBs, ATM is activated through a series of events:

Detection of DNA Breaks: ATM can sense DNA breaks by associating with the MRN complex (MRE11, RAD50, and NBS1). This complex recognizes DSBs, leading to ATM's recruitment to the damaged site.

Autophosphorylation: Upon detection of DNA damage, ATM undergoes autophosphorylation at serine 1981 (S1981), leading to its activation. This phosphorylation event is critical for ATM's kinase activity and its ability to phosphorylate downstream targets.

Dimer-to-Monomer Transition: In its inactive form, ATM is a dimer. It transitions to an active monomeric state upon activation, allowing it to interact with and phosphorylate various downstream proteins.

Phosphorylation Targets of ATM

Once activated, ATM phosphorylates many proteins involved in the DNA damage response, cell cycle regulation, and apoptosis. Here are some critical targets of ATM:

CHK2: ATM phosphorylates CHK2, a cell cycle checkpoint control kinase. This phosphorylation helps to halt the cell cycle, allowing time for DNA repair.

p53: ATM phosphorylates p53, activating this tumor suppressor, leading to cell cycle arrest or apoptosis if the damage is irreparable.

H2AX: ATM phosphorylates histone H2AX, forming γ-H2AX, a marker of DNA damage. This modification helps signal the presence of DSBs and recruit DNA repair machinery.

BRCA1: ATM's phosphorylation of BRCA1 is critical for homologous recombination, a key DNA repair pathway for DSBs.

NBS1: As part of the MRN complex, NBS1 phosphorylation by ATM enhances the complex's DNA repair functions.

53BP1: ATM phosphorylation of 53BP1 helps recruit this protein to sites of DSBs, guiding repair pathways like non-homologous end joining (NHEJ).

Role of ATM Phosphorylation in DNA Repair

ATM-mediated phosphorylation plays a central role in coordinating the DNA damage response:

Signal Propagation: Phosphorylation cascades initiated by ATM amplify the signal for DNA damage, ensuring an efficient response.

Recruitment of Repair Machinery: Phosphorylation of specific proteins helps recruit DNA repair complexes to the sites of DNA damage.

Cell Cycle Regulation: ATM's activation can lead to cell cycle checkpoints, preventing cells from dividing with damaged DNA.

Apoptosis: If the DNA damage is too severe to repair, ATM's activation can lead to apoptosis, preventing the propagation of damaged cells

ATM's phosphorylation in response to DNA damage is crucial for detecting DNA double-strand breaks and coordinating the DNA damage response. By phosphorylating a range of critical proteins, ATM orchestrates a complex network of signaling events that facilitate DNA repair, cell cycle regulation, and apoptosis, thereby maintaining genomic stability.

Method

HeLa cells were grown on acid-etched #1.5H cover glass to ~50% confluency. DNA damage was induced by treatment with 2 µM etoposide-spiked complete growth media for 12 hours, followed by fixation in -20 °C methanol and blocking with Thermo Fisher Fish Serum Blocker (cat#37527X3). The primary antibody, Rabbit anti-Human ATM.p (Serine 1981) Recombinant Monoclonal - Identifyn® SRM Alexa Fluor™ 647, IgG - (BLR031P), was incubated for 1 hour at room temperature at a 1:250 dilution. Cells were washed 5 times in 1X PBS and mounted using ProLong™ Diamond Antifade Mountant with DAPI (cat# P36962).

Control Data - Primary Unconjugated Antibody

Microscope

Zeiss Axio Imager.M1 Widefield, using a Plan-Apochromat 63x/1.40 Oil M27, Axiocam 705, and X-Cite Xylis Lamp, was used with the following parameters for each dye:

Single Plane (2D)

Channels = 2
Scaling (Per Pixel) = 0.110 µm X 0.110 µm
Image Size (Pixels) = 711 X 636
Image Size (Scaled) = 77.87 µm X 69.66 µm
Bit Depth = 14 Bit
Image Center Position = X: 0.00 µm, Y: 0.00 µm
ROI Center Offset = X: 0.00 µm, Y: 0.00 µm

647 -

Reflector = 50 Cy 5
Beam Splitter = 660
Filter Excitation Wavelength = 625 - 655
Filter Emission Wavelength = 665 - 715
Contrast Method = Fluorescence
Light Source = X-Cite Xylis Lamp Intensity @ 25.00%
Exposure Time = 250 ms
Excitation Wavelength = 653
Emission Wavelength = 668
Effective NA = 1.4
Imaging Device = Axiocam 705
Camera Adapter = 1x Camera Adapter
Depth of Focus = 1.03 µm
Binning Mode = 2,2

DAPI -

Reflector = 49 DAPI
Beam Splitter = 395
Filter Excitation Wavelength = 335 - 383
Filter Emission Wavelength = 420 - 470
Contrast Method = Fluorescence
Light Source = X-Cite Xylis Lamp Intensity @ 10.00%
Exposure Time = 25 ms
Excitation Wavelength = 353
Emission Wavelength = 465
Effective NA = 1.4
Imaging Device = Axiocam 705
Camera Adapter = 1x Camera Adapter
Depth of Focus = 0.72 µm
Binning Mode = 2,2

Split View - Panel A

The left panel shows Rabbit anti-Human ATM.p Recombinant Monoclonal - Identifyn® SRM Alexa Fluor™ 647, IgG - (BLR031P). The middle panel shows DAPI nuclear counterstaining. The right panel shows the merged image, demonstrating strong nuclear localization and discrete ATM.p foci formation following DNA damage induction, supporting robust conjugation performance and preservation of target-specific signal under widefield fluorescence microscopy conditions.

ZEN Acquisition Info Tab - Panel B

Shown is the acquisition interface for the Rabbit anti-Human Phospho- ATM (Serine 1981) Recombinant Monoclonal - Identifyn® SRM Alexa Fluor™ 647, IgG - (BLR031P) widefield dataset collected using the X-Cite Xylis Lamp and Zeiss Axiocam 705 camera. Imaging was performed using only 25% X-Cite Xylis Lamp intensity with a 250 ms exposure time on the Axiocam 705, demonstrating robust signal generation under standard widefield excitation and collection conditions. The ability to generate a strong nuclear-associated ATM.p signal and to form discrete foci under these moderate acquisition settings supports the robustness of direct conjugation and the preservation of biologically relevant localization characteristics. These findings further demonstrate that fluorescence intensity was achieved without reliance on excessive excitation power or prolonged exposure conditions.

2.5D Image Processing - Panel C

2.5D Display

Render Mode = Surface
Grid distance = 5
Palette and Show Faces at Side are both Selected

2.5D Display Options

Angle X = 54
Angle Y = -180
Z Scaling = 1.0
Ambient = 50
Specular = 20
Shininess = 50
Light Height = 2.0

ZEN Acquisition Histogram Data - Panel C

Shown is the maximum fluorescence intensity measurement obtained from the Zeiss ZEN Histogram tool for the Rabbit anti-Human ATM.p Recombinant Monoclonal - Identifyn® SRM Alexa Fluor™ 647, IgG - (BLR031P) direct conjugate, demonstrating a peak signal intensity of 5,188.000 A.U., supporting robust fluorophore conjugation and strong signal generation under standard widefield acquisition conditions.

Summary

Panel A depicts widefield fluorescence microscopy of the Rabbit anti-Human ATM.p Recombinant Monoclonal - Identifyn® SRM Alexa Fluor™ 647, IgG - (BLR031P) following DNA damage induction. The left panel shows direct localization of the ATM.p signal, the middle panel shows DAPI nuclear counterstaining, and the right panel shows the merged image. Strong nuclear-associated fluorescence and discrete punctate foci formation were observed throughout the nuclei of damaged cells, demonstrating effective target localization and preservation of signal integrity following direct conjugation. Signal distribution remained well resolved with minimal nonspecific background fluorescence, allowing clear visualization of ATM.p-associated nuclear structures under standard widefield imaging conditions. These observations are consistent with the corresponding unconjugated stepdown dataset generated using Rabbit anti-Human ATM.p Recombinant Monoclonal, IgG - (BLR031P) (Cat ID# - PA-RR 000012), supporting equivalent staining behavior, preservation of antibody performance characteristics, and robust fluorophore conjugation efficiency.

Panel B shows the Zeiss ZEN acquisition interface and associated imaging parameters utilized during image collection. Widefield excitation was performed using the X-Cite Xylis Lamp at 25% lamp intensity, while fluorescence collection was performed with the Zeiss Axiocam 705 camera using a 250 ms exposure time. These moderate acquisition settings yielded strong signal intensity, clear nuclear resolution, and discrete ATM.p-associated foci formation without requiring excessive excitation power or prolonged exposure conditions. Importantly, the acquisition parameters closely mirrored those required for the corresponding unconjugated primary antibody workflow, further supporting preservation of signal strength, fluorophore stability, and overall conjugation performance following direct labeling with Identifyn® SRM Alexa Fluor™ 647. The ability to maintain robust signal generation under conventional widefield fluorescence microscopy conditions supports the utility of the direct conjugate for routine fluorescence imaging applications.

Panel C presents a 2.5D fluorescence intensity representation generated from the acquired widefield dataset. Intensity mapping demonstrated strong nuclear localization and pronounced ATM.p-associated foci formation in association with DAPI-positive nuclei, with elevated fluorescence peaks corresponding to discrete regions of ATM.p accumulation.

The 2.5D reconstruction further illustrates the dynamic intensity variation across the nuclear landscape and supports the visual interpretation of robust target-associated fluorescence signal generation. Quantitative analysis performed with the Zeiss ZEN histogram tool showed a maximum fluorescence intensity of 5,188.000 A.U., further supporting the robustness of the conjugation under standard widefield LED excitation and collection parameters. Collectively, these findings demonstrate that the direct conjugate maintains strong signal generation, nuclear specificity, low background interference, and compatibility with conventional widefield fluorescence microscopy workflows, while preserving imaging characteristics comparable to those of the unconjugated antibody workflow.

Image Correction

NONE

Image by E.F.Simon
Image Analysis and Data Presentation by B.T. Bennett

SOURCE PROVENANCE

Catalog	DC-000074
Stage	Widefield
Instrument	ZEISS Axio Imager.M1
Microscope configuration	Zeiss Axio Imager.M1 Widefield, using a Plan-Apochromat 63x/1.40 Oil M27, Axiocam 705, and X-Cite Xylis Lamp, was used with the following parameters for each dye:
Structured source metadata values	39
Metadata source	PRESERVED_SOURCE_METHOD_PDF_TEXT
Cell model	HeLa
Image SHA-256	A7D06F26F9A6F224CE73945BCFC3C49BC95D80D27D1D8E981BBC5CB0F2BA70E4
Method PDF SHA-256	A98E6F2788B8E9D8DF514D7D64165B10B8A8C3971CE8EC0BA569A4909178347E

ORIGINAL IMAGE EVIDENCE / CONFOCAL

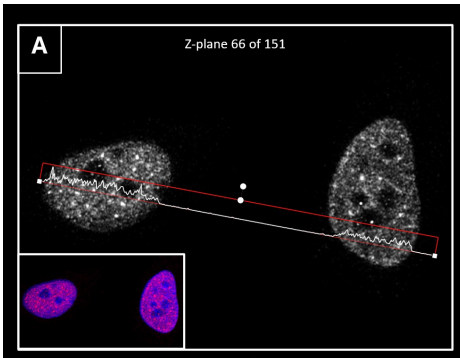

Rabbit anti-Human Phospho- ATM (Serine 1981) Recombinant Monoclonal - Identifyn® SRM Alexa Fluor™ 647, IgG – (BLR031P). Line profile analysis is shown, with the 647-channel displayed in white to enhance visualization of signal distribution and fluorescence intensity across the line profile. The lower left panel shows the same z-plane displayed in the default 647 pseudo color (red) alongside DAPI nuclear counterstaining.

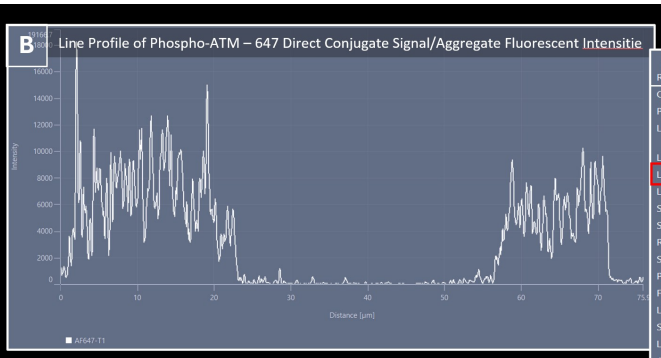

Maximum Foci Aggregate 18,252.00 A.U. @ 2.00 % laser Input

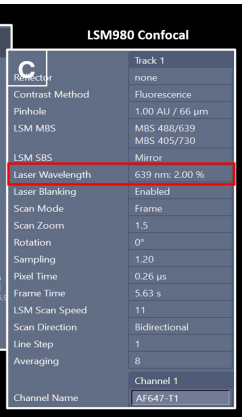

Panel A depicts confocal fluorescence microscopy of the Rabbit anti-Human ATM.p (Serine 1981) Recombinant Monoclonal - Identifyn® SRM Alexa Fluor™ 647, IgG – (BLR031P) acquired on the Zeiss LSM 980 Confocal microscope at z-plane 66 of 151 following DNA damage induction. The primary image displays the 647-channel rendered in white to enhance visualization of signal distribution and fluorescence intensity along the selected line profile. A line profile overlay shows localized changes in fluorescence intensity across the measured region of interest. In the lower-left corner of Panel A, the same z-plane is additionally shown with ATM.p displayed in its default 647 pseudo color (red) alongside DAPI nuclear counterstaining, demonstrating strong nuclear-associated localization, discrete foci formation, and preservation of robust signal integrity following direct conjugation. Signal distribution and staining characteristics were consistent with the corresponding unconjugated stepdown dataset generated using Rabbit anti-Human ATM.p (Serine 1981) Recombinant Monoclonal, IgG – (BLR031P) (Cat ID# - PA-RR 000012), supporting equivalent localization behavior and fluorophore performance following direct labeling with Identifyn® SRM Alexa Fluor™ 647.

Panel B presents the fluorescence intensity line profile graph generated from the selected measurement region shown in Panel A. The graph demonstrates localized variation in fluorescence intensity across the sampled nuclei, with pronounced signal peaks corresponding to ATM.p-associated foci formation within damaged nuclei. Importantly, the line profile traverses two nuclei, clearly demonstrating nuclear-specific localization and target-associated fluorescence enrichment following DNA damage induction. Quantitative analysis demonstrated a maximum fluorescence intensity of 18,252.00 A.U., supporting the robustness of the conjugation and strong signal generation under standard confocal acquisition conditions.

Panel C shows the Zeiss ZEN acquisition interface and associated imaging parameters utilized during confocal image collection. Imaging was performed using the 639 nm laser line at only 2.00 % laser power, demonstrating that a strong fluorescence signal and clear nuclear resolution were achieved without excessive excitation conditions. These moderate acquisition settings further support the vigor of direct conjugation, fluorophore efficiency, and signal preservation following direct labeling with Identifyn® SRM Alexa Fluor™ 647. Collectively, the dataset demonstrates robust nuclear-associated ATM.p signal generation, discrete foci resolution, and compatibility with high-resolution confocal fluorescence microscopy workflows.

Rabbit anti-Human ATM.p (Serine 1981) Recombinant Monoclonal - Identifyn® SRM Alexa Fluor™ 647, IgG - (BLR031P)
Cat ID# - DC 000074

EVIDENCE TIER	Confocal
INSTRUMENT	ZEISS LSM 980
CELL MODEL	HeLa
DETECTED DYES	405/DAPI; 488; 647
METADATA VALUES	44

STRUCTURED ACQUISITION METADATA / CONFOCAL

The values below were deterministically extracted from the preserved Identifyn method PDF text. They remain source-documented metadata, not new BENNETT measurements.

FIELD	SOURCE-DOCUMENTED VALUE
Platform / configuration	Zeiss LSM 980 Confocal with NIR Detection, Axio Observer.Z1/7, using a Plan-Apochromat 63x/1.40 Oil DIC M27, was used with the following parameters for each dye:
Objective	Plan-Apochromat 63x/1.40 Oil DIC M27
Z-Stack	151 Slices (4.5 µm)
Channels	2
Scaling (Per Pixel)	0.059 µm X 0.059 µm X 0.030 µm
Image Size (Pixels)	1406 X 1041
Image Size (Scaled)	82.68 µm X 61.21 µm
Bit Depth	16 Bit
Image Center Position	X: 80.57 mm, Y: 50.66 mm
Stage Position	X: 80.57 mm, Y: 50.66 mm
ROI Center Offset	X: 0.00 µm, Y: 0.00 µm
Reflector	None
Contrast Method	Fluorescence
Pinhole	1.00 AU / 66 µm | 1.00 AU / 44 µm
LMS MBS	MBS 488/639 & 405/730
LMS SBS	Mirror
Laser Wavelength	639 nm @ 2.00% | 405 nm @ 0.8%
Laser Blanking	Enabled
Scan Mode	Frame
Scan Zoom	1.5
Rotation	0°
Sampling	1.20
Pixel Time	0.26 µs
Frame Time	5.63 s
LSM Scan Speed	11
Scan Direction	Bidirectional
Line Step	1
Averaging	8
Excitation Wavelength	653 | 353
Emission Wavelength	668 | 465
Effective NA	1.4
Detection Wavelength	635 - 745 | 430 - 490
Imaging Device	GaAsP-Pmt3

FIELD	SOURCE-DOCUMENTED VALUE
Detector Type	GaAsP-PMT
Detector Gain	500 V
Detector Offset	0
Detector Digital Gain	1.0
LSM Plus Mode	Filter: 7.8 (3D, Auto) | Filter: 6.8 (3D, Auto)
Profile Definition	Stroke Thickness 1.5, Normal View, Grid Distance 1
Profile View	X and Y axes were set to Auto - X (Min 0.0 and Max 75.9), Y (Min 0 and Max 19167)

SOURCE METHOD

The text below is carried from the preserved Identifyn source record. Typography and pagination have been normalized for this preservation dossier; scientific wording has not been editorially rewritten.

Identifyn Standards for Optical Microscopy Methods™

Identifyn® Primary Antibody

Rabbit anti-Human ATM.p (Serine 1981) Recombinant Monoclonal - Identifyn® SRM Alexa Fluor™ 647, IgG - (BLR031P)
Cat ID# - DC 000074

ATM (ataxia-telangiectasia mutated) is a crucial serine/threonine kinase that plays a central role in the DNA damage response (DDR), particularly in response to DNA double-strand breaks (DSBs). ATM's activation and subsequent phosphorylation cascades are essential for detecting DNA damage and initiating repair processes. Here's a detailed overview of how ATM is activated, its targets, and its role in the DDR:

Activation of ATM
In response to DNA damage, particularly DSBs, ATM is activated through a series of events:

Detection of DNA Breaks: ATM can sense DNA breaks by associating with the MRN complex (MRE11, RAD50, and NBS1). This complex recognizes DSBs, leading to ATM's recruitment to the damaged site.

Autophosphorylation: Upon detection of DNA damage, ATM undergoes autophosphorylation at serine 1981 (S1981), leading to its activation. This phosphorylation event is critical for ATM's kinase activity and its ability to phosphorylate downstream targets.

Dimer-to-Monomer Transition: In its inactive form, ATM is a dimer. It transitions to an active monomeric state upon activation, allowing it to interact with and phosphorylate various downstream proteins.

Phosphorylation Targets of ATM

Once activated, ATM phosphorylates many proteins involved in the DNA damage response, cell cycle regulation, and apoptosis. Here are some critical targets of ATM:

CHK2: ATM phosphorylates CHK2, a cell cycle checkpoint control kinase. This phosphorylation helps to halt the cell cycle, allowing time for DNA repair.

p53: ATM phosphorylates p53, activating this tumor suppressor, leading to cell cycle arrest or apoptosis if the damage is irreparable.

H2AX: ATM phosphorylates histone H2AX, forming γ-H2AX, a marker of DNA damage. This modification helps signal the presence of DSBs and recruit DNA repair machinery.

BRCA1: ATM's phosphorylation of BRCA1 is critical for homologous recombination, a key DNA repair pathway for DSBs.

NBS1: As part of the MRN complex, NBS1 phosphorylation by ATM enhances the complex's DNA repair functions.

53BP1: ATM phosphorylation of 53BP1 helps recruit this protein to sites of DSBs, guiding repair pathways like non-homologous end joining (NHEJ).

Role of ATM Phosphorylation in DNA Repair

ATM-mediated phosphorylation plays a central role in coordinating the DNA damage response:

Signal Propagation: Phosphorylation cascades initiated by ATM amplify the signal for DNA damage, ensuring an efficient response.

Recruitment of Repair Machinery: Phosphorylation of specific proteins helps recruit DNA repair complexes to the sites of DNA damage.

Cell Cycle Regulation: ATM's activation can lead to cell cycle checkpoints, preventing cells from dividing with damaged DNA.

Apoptosis: If the DNA damage is too severe to repair, ATM's activation can lead to apoptosis, preventing the propagation of damaged cells

ATM's phosphorylation in response to DNA damage is crucial for detecting DNA double-strand breaks and coordinating the DNA damage response. By phosphorylating a range of critical proteins, ATM orchestrates a complex network of signaling events that facilitate DNA repair, cell cycle regulation, and apoptosis, thereby maintaining genomic stability.

Methods

HeLa cells were grown on acid-etched #1.5H cover glass to ~50% confluency. DNA damage was induced by treatment with 2 µM etoposide-spiked complete growth media for 12 hours, followed by fixation in -20 °C methanol and blocking with Thermo Fisher Fish Serum Blocker (cat#37527X3). The primary antibody, Rabbit anti-Human ATM.p (Serine 1981) Recombinant Monoclonal - Identifyn® SRM Alexa Fluor™ 647, IgG - (BLR031P), was incubated for 1 hour at room temperature at a 1:250 dilution. Cells were washed 5X in PBS and mounted using ProLong™ Diamond Antifade Mountant with DAPI (cat# P36962).

Control Data - Primary Unconjugated Antibody

Microscope

Zeiss LSM 980 Confocal with NIR Detection, Axio Observer.Z1/7, using a Plan-Apochromat 63x/1.40 Oil DIC M27, was used with the following parameters for each dye:

Z Stack - (3D) - Panels A and B, Z-plane 66 of 151

Z-Stack = 151 Slices (4.5 µm)

Channels = 2
Scaling (Per Pixel) = 0.059 µm X 0.059 µm X 0.030 µm
Image Size (Pixels) = 1406 X 1041
Image Size (Scaled) = 82.68 µm X 61.21 µm
Bit Depth = 16 Bit
Image Center Position = X: 80.57 mm, Y: 50.66 mm
Stage Position = X: 80.57 mm, Y: 50.66 mm
ROI Center Offset = X: 0.00 µm, Y: 0.00 µm

647 -

Reflector = None
Contrast Method = Fluorescence
Pinhole = 1.00 AU / 66 µm
LMS MBS = MBS 488/639 & 405/730
LMS SBS = Mirror
Laser Wavelength = 639 nm @ 2.00%
Laser Blanking = Enabled
Scan Mode = Frame
Scan Zoom = 1.5
Rotation = 0°
Sampling = 1.20
Pixel Time = 0.26 µs
Frame Time = 5.63 s
LSM Scan Speed = 11
Scan Direction = Bidirectional
Line Step = 1
Averaging = 8
Excitation Wavelength = 653
Emission Wavelength = 668
Effective NA = 1.4
Detection Wavelength = 635 - 745
Imaging Device = GaAsP-Pmt3
Detector Type = GaAsP-PMT
Detector Gain = 500 V
Detector Offset = 0
Detector Digital Gain = 1.0
LSM Plus Mode = Filter: 7.8 (3D, Auto)

DAPI -

Reflector = None
Contrast Method = Fluorescence
Pinhole = 1.00 AU / 44 µm
LMS MBS = MBS 488/639 & 405/730
LMS SBS = Mirror
Laser Wavelength = 405 nm @ 0.8%
Laser Blanking = Enabled
Scan Mode = Frame
Scan Zoom = 1.5
Rotation = 0°
Sampling = 1.20
Pixel Time = 0.26 µs
Frame Time = 5.63 s
LSM Scan Speed = 11
Scan Direction = Bidirectional
Line Step = 1
Averaging = 8
Excitation Wavelength = 353
Emission Wavelength = 465
Effective NA = 1.4
Detection Wavelength = 430 - 490
Imaging Device = GaAsP-Pmt3
Detector Type = GaAsP-PMT
Detector Gain = 500 V
Detector Offset = 0
Detector Digital Gain = 1.0
LSM Plus Mode = Filter: 6.8 (3D, Auto)

2-Dimensional View - Panel A

Rabbit anti-Human ATM.p (Serine 1981) Recombinant Monoclonal - Identifyn® SRM Alexa Fluor™ 647, IgG - (BLR031P) acquired on the Zeiss LSM 980 Confocal microscope at z-plane 66 of 151 following DNA damage induction. The primary image displays the 647 channel rendered in white to enhance visualization of signal distribution and fluorescence intensity along the selected line profile. The lower-left inset shows the same z-plane displayed in the default 647 pseudocolor (red) alongside DAPI nuclear counterstaining, demonstrating strong nuclear-associated localization, discrete ATM.p foci formation, and robust signal generation following direct conjugation.

Profile View Display - Panel B

Profile Definition = Stroke Thickness 1.5, Normal View, Grid Distance 1
Profile View = X and Y axes were set to Auto - X (Min 0.0 and Max 75.9), Y (Min 0 and Max 19167)

ZEN Acquisition Info Tab - Panel C

Shown is the acquisition of the 647 channel (Phospho-ATM 647 direct conjugate) using the 639 nm laser at 2.00%, demonstrating that image acquisition settings do not artificially produce the signal.

Summary

Panel A depicts confocal fluorescence microscopy of the Rabbit anti-Human ATM.p Recombinant Monoclonal - Identifyn® SRM Alexa Fluor™ 647, IgG - (BLR031P) acquired on the Zeiss LSM 980 Confocal microscope at z-plane 66 of 151 following DNA damage induction. The primary image displays the 647 channel rendered in white to enhance visualization of signal distribution and fluorescence intensity along the selected line profile. A line profile overlay shows localized changes in fluorescence intensity across the measured region of interest. In the lower-left corner of Panel A, the same z-plane is additionally shown with ATM.p displayed in its default 647 pseudocolor (red) alongside DAPI nuclear counterstaining, demonstrating strong nuclear-associated localization, discrete foci formation, and preservation of robust signal integrity following direct conjugation. Signal distribution and staining characteristics were consistent with the corresponding unconjugated stepdown dataset generated using Rabbit anti-Human ATM.p Recombinant Monoclonal, IgG - (BLR031P) (Cat ID# - PA-RR 000012), supporting equivalent localization behavior and fluorophore performance following direct labeling with Identifyn® SRM Alexa Fluor™ 647.

Panel B presents the fluorescence-intensity line profile generated from the selected measurement region shown in Panel A. The graph demonstrates localized variation in fluorescence intensity across the sampled nuclei, with pronounced signal peaks corresponding to ATM.p-associated foci formation within damaged nuclei. Importantly, the line profile traverses two nuclei, clearly demonstrating nuclear-specific localization and target-associated fluorescence enrichment following DNA damage induction. Quantitative analysis demonstrated a maximum fluorescence intensity of 18,252.00 A.U., supporting the robustness of the conjugation and strong signal generation under standard confocal acquisition conditions.

Panel C shows the Zeiss ZEN acquisition interface and associated imaging parameters utilized during confocal image collection. Imaging was performed using the 639 nm laser line at only 2.00% laser power, demonstrating that a strong fluorescence signal and clear nuclear resolution were achieved without excessive excitation conditions. These moderate acquisition settings further support the vigor of direct conjugation, the efficiency of fluorophores, and the preservation of signal following direct labeling with Identifyn® SRM Alexa Fluor™ 647. Collectively, the dataset demonstrates robust nuclear-associated ATM.p signal generation, discrete foci resolution, and compatibility with high-resolution confocal fluorescence microscopy workflows.

Image Correction

NONE

Image by J.K. Bennett
Image Analysis and Data Presentation by B.T. Bennett

SOURCE PROVENANCE

Catalog	DC-000074
Stage	Confocal
Instrument	ZEISS LSM 980
Microscope configuration	Zeiss LSM 980 Confocal with NIR Detection, Axio Observer.Z1/7, using a Plan-Apochromat 63x/1.40 Oil DIC M27, was used with the following parameters for each dye:
Structured source metadata values	44
Metadata source	PRESERVED_SOURCE_METHOD_PDF_TEXT

SOURCE PROVENANCE

Cell model	HeLa
Image SHA-256	66F059C2F2CEDABD6AAED9678DD2F599CBD28C10E29B418082645B74D42DF5AD
Method PDF SHA-256	430D3C9C90B10F7BBCE9839210CF84674D87FE4BAF35755FCBBD624F62DF56EA

ORIGINAL IMAGE EVIDENCE / AIRYSCAN

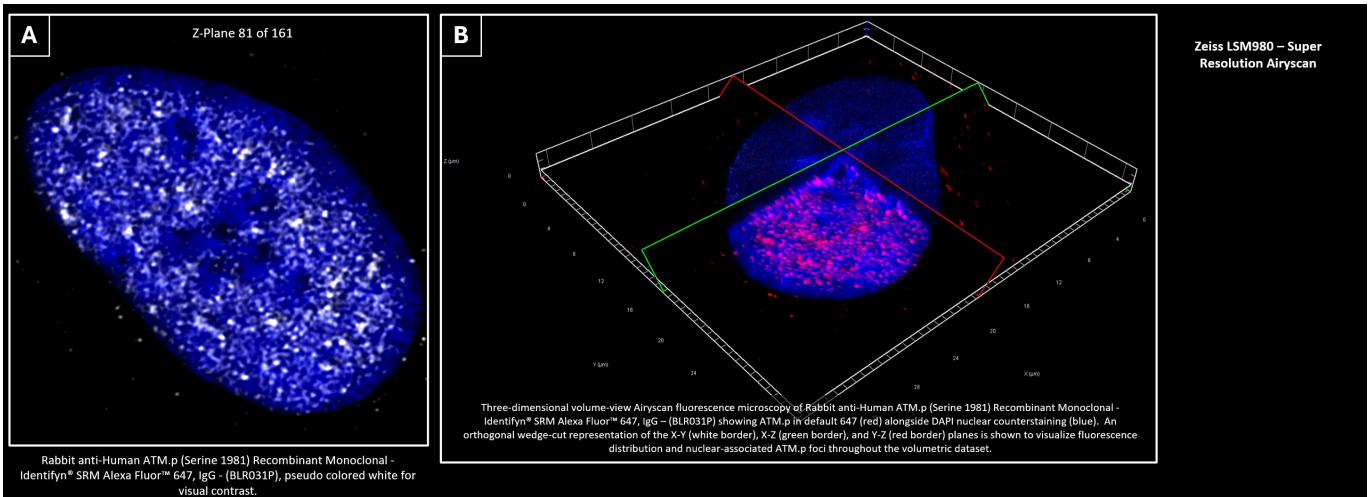

EVIDENCE TIER	Airyscan
INSTRUMENT	ZEISS LSM 980
CELL MODEL	HeLa
DETECTED DYES	405/DAPI; 488; 647
METADATA VALUES	57

STRUCTURED ACQUISITION METADATA / AIRYSCAN

The values below were deterministically extracted from the preserved Identifyn method PDF text. They remain source-documented metadata, not new BENNETT measurements.

FIELD	SOURCE-DOCUMENTED VALUE
Platform / configuration	Zeiss LSM 980 Confocal with NIR Detection, Axio Observer.Z1/7, using a Plan-Apochromat 63x/1.40 Oil DIC M27, was used with the following parameters for each dye:
Objective	Plan-Apochromat 63x/1.40 Oil DIC M27
Z-Stack	161 Slices (4.8 µm)
Channels	3
Scaling (Per Pixel)	0.03530 µm X 0.03530 µm X 0.03000 µm
Image Size (Pixels)	1045 X 937
Image Size (Scaled)	36.88 µm X 33.07 µm
Bit Depth	16 Bit
Image Center Position	X: 79.75 mm, Y: 50.77 mm
Stage Position	X: 79.75 mm, Y: 50.77 mm
ROI Center Offset	X: 0.00 µm, Y: 0.00 µm
Reflector	None
Contrast Method	Fluorescence
Pinhole	5.00 AU / 328 µm | 5.00 AU / 215 µm
LMS MBS	MBS 488/639 & 405/730
LMS SBS	SBS LP 640 | SBS SP 505
Laser Wavelength	639 nm @ 1.10% | 405 nm @ 1.0%
Laser Blanking	Enabled
Scan Mode	Frame
Scan Zoom	2.0
Rotation	0°
Sampling	2.00
Pixel Time	1.10 µs
Frame Time	18.77 s
LSM Scan Speed	6
Scan Direction	Bidirectional
Line Step	1
Averaging	4
Excitation Wavelength	653 | 353
Emission Wavelength	668 | 465
Effective NA	1.4
Detection Wavelength	643 - 745 | 350 - 499
Imaging Device	Airyscan

FIELD	SOURCE-DOCUMENTED VALUE
Detector Type	GaAsP-PMT
Detector Gain	800 V
Detector Offset	0
Detector Digital Gain	1.0
Airyscan Mode	Super Resolution: 10.0 (3D, Auto) | Super Resolution: 8.9 (3D, Auto)
3D Volume Projection	Precise
Appearance	Threshold 2% all channels, Ramp 98% all channels, Maximum 100% all channels
Background	Black
Light	Brightness 100%, Azimuth 80°, Elongation -130°, Enabled Directional Lighting, Enabled Tone Mapping
Projection	View Angle 35°, Scale Z 100%, Reverse Z-Axis NOT Selected, Stereo Anaglyph NOT Selected, Camera Separation 5% (deselected), Parallax Shift 0% (deselected)
X-Y	Activate was selected, textured opaque was chosen, and a white outline of the clipped perimeter was shown; Clip Back was selected, and Clip Front was NOT selected.
Position of Clip	-38% | 0%
Clip X	0°
Clip Z	0°
X-Z	Activate was selected, textured opaque was chosen, and a green outline of the clipped perimeter was shown; Clip Back was selected, and Clip Front was NOT selected.
Clip Y	45° | -45°
Y-Z	Activate was selected, textured opaque was chosen, and a red outline of the clipped perimeter was shown; Clip Back was selected, and Clip Front was NOT selected.

SOURCE METHOD

The text below is carried from the preserved Identifyn source record. Typography and pagination have been normalized for this preservation dossier; scientific wording has not been editorially rewritten.

Identifyn Standards for Optical Microscopy Methods™

Identifyn® Primary Antibody

Rabbit anti-Human ATM.p (Serine 1981) Recombinant Monoclonal - Identifyn® SRM Alexa Fluor™ 647, IgG - (BLR031P)
Cat ID# - DC 000074

ATM (ataxia-telangiectasia mutated) is a crucial serine/threonine kinase that plays a central role in the DNA damage response (DDR), particularly in response to DNA double-strand breaks (DSBs). ATM's activation and subsequent phosphorylation cascades are essential for detecting DNA damage and initiating repair processes. Here's a detailed overview of how ATM is activated, its targets, and its role in the DDR:

Activation of ATM

In response to DNA damage, particularly DSBs, ATM is activated through a series of events:

Detection of DNA Breaks: ATM can sense DNA breaks by associating with the MRN complex (MRE11, RAD50, and NBS1). This complex recognizes DSBs, leading to ATM's recruitment to the damaged site.

Autophosphorylation: Upon detection of DNA damage, ATM undergoes autophosphorylation at serine 1981 (S1981), leading to its activation. This phosphorylation event is critical for ATM's kinase activity and its ability to phosphorylate downstream targets.

Dimer-to-Monomer Transition: In its inactive form, ATM is a dimer. It transitions to an active monomeric state upon activation, allowing it to interact with and phosphorylate various downstream proteins.

Phosphorylation Targets of ATM

Once activated, ATM phosphorylates many proteins involved in the DNA damage response, cell cycle regulation, and apoptosis. Here are some critical targets of ATM:

CHK2: ATM phosphorylates CHK2, a cell cycle checkpoint control kinase. This phosphorylation helps to halt the cell cycle, allowing time for DNA repair.

p53: ATM phosphorylates p53, activating this tumor suppressor, leading to cell cycle arrest or apoptosis if the damage is irreparable.

H2AX: ATM phosphorylates histone H2AX, forming γ-H2AX, a marker of DNA damage. This modification helps signal the presence of DSBs and recruit DNA repair machinery.

BRCA1: ATM's phosphorylation of BRCA1 is critical for homologous recombination, a key DNA repair pathway for DSBs.

NBS1: As part of the MRN complex, NBS1 phosphorylation by ATM enhances the complex's DNA repair functions.

53BP1: ATM phosphorylation of 53BP1 helps recruit this protein to sites of DSBs, guiding repair pathways like non-homologous end joining (NHEJ).

Role of ATM Phosphorylation in DNA Repair

ATM-mediated phosphorylation plays a central role in coordinating the DNA damage response:

Signal Propagation: Phosphorylation cascades initiated by ATM amplify the signal for DNA damage, ensuring an efficient response.

Recruitment of Repair Machinery: Phosphorylation of specific proteins helps recruit DNA repair complexes to the sites of DNA damage.

Cell Cycle Regulation: ATM activation can lead to cell cycle checkpoints, preventing cells with damaged DNA from dividing.

Apoptosis: If the DNA damage is too severe to repair, ATM's activation can lead to apoptosis, preventing the propagation of damaged cells

ATM's phosphorylation in response to DNA damage is crucial for detecting DNA double-strand breaks and coordinating the DNA damage response. By phosphorylating a range of critical proteins, ATM orchestrates a complex network of signaling events that facilitate DNA repair, cell cycle regulation, and apoptosis, thereby maintaining genomic stability.

Methods

HeLa cells were grown on acid-etched #1.5H cover glass to ~50% confluency. DNA damage was induced by treatment with 2 µM etoposide-spiked complete growth media for 12 hours, followed by fixation in -20 °C methanol and blocking with Thermo Fisher Fish Serum Blocker (cat#37527X3). The primary antibody, Rabbit anti-Human ATM.p (Serine 1981) Recombinant Monoclonal - Identifyn® SRM Alexa Fluor™ 647, IgG - (BLR031P), was incubated for 1 hour at room temperature at a 1:250 dilution. Cells were washed 5 times in 1X PBS and mounted using ProLong™ Diamond Antifade Mountant with DAPI (cat# P36962).

Control Data - Primary Unconjugated Antibody

Microscope

Zeiss LSM 980 Confocal with NIR Detection, Axio Observer.Z1/7, using a Plan-Apochromat 63x/1.40 Oil DIC M27, was used with the following parameters for each dye:

Z Stack - (3D) - Panel A, Z-Plane 81 of 161 & Panel B, 3-Dimensional Volume View

Z-Stack = 161 Slices (4.8 µm)

Channels = 3
Scaling (Per Pixel) = 35.30 nm X 35.30 nm X 30.00 nm
Image Size (Pixels) = 1045 X 937
Image Size (Scaled) = 36.88 µm X 33.07 µm
Bit Depth = 16 Bit
Image Center Position = X: 79.75 mm, Y: 50.77 mm
Stage Position = X: 79.75 mm, Y: 50.77 mm
ROI Center Offset = X: 0.00 µm, Y: 0.00 µm

647 -

Reflector = None
Contrast Method = Fluorescence
Pinhole = 5.00 AU / 328 µm
LMS MBS = MBS 488/639 & 405/730
LMS SBS = SBS LP 640
Laser Wavelength = 639 nm @ 1.10%
Laser Blanking = Enabled
Scan Mode = Frame
Scan Zoom = 2.0
Rotation = 0°
Sampling = 2.00
Pixel Time = 1.10 µs
Frame Time = 18.77 s
LSM Scan Speed = 6
Scan Direction = Bidirectional
Line Step = 1
Averaging = 4
Excitation Wavelength = 653
Emission Wavelength = 668
Effective NA = 1.4
Detection Wavelength = 643 - 745
Imaging Device = Airyscan
Detector Type = GaAsP-PMT
Detector Gain = 800 V
Detector Offset = 0
Detector Digital Gain = 1.0
Airyscan Mode = Super Resolution: 10.0 (3D, Auto)

DAPI -

Reflector = None
Contrast Method = Fluorescence
Pinhole = 5.00 AU / 215 µm
LMS MBS = MBS 488/639 & 405/730
LMS SBS = SBS SP 505
Laser Wavelength = 405 nm @ 1.0%
Laser Blanking = Enabled
Scan Mode = Frame
Scan Zoom = 2.0
Rotation = 0°
Sampling = 2.00
Pixel Time = 1.10 µs
Frame Time = 18.77 s
LSM Scan Speed = 6
Scan Direction = Bidirectional
Line Step = 1
Averaging = 4
Excitation Wavelength = 353
Emission Wavelength = 465
Effective NA = 1.4
Detection Wavelength = 350 - 499
Imaging Device = Airyscan
Detector Type = GaAsP-PMT
Detector Gain = 800 V
Detector Offset = 0
Detector Digital Gain = 1.0
Airyscan Mode = Super Resolution: 8.9 (3D, Auto)

2-Dimensional View - Panel A

Panel A depicts Airyscan super-resolution fluorescence microscopy of Rabbit anti-Human ATM.p (Serine 1981) Recombinant Monoclonal - Identifyn® SRM Alexa Fluor™ 647, IgG - (BLR031P) acquired at z-plane 81 of 161 following DNA damage induction. The ATM.p signal is pseudocolored white to enhance visual contrast, demonstrating strong nuclear localization, discrete ATM.p-associated foci formation, and robust signal integrity, consistent with the corresponding unconjugated, widefield, and confocal datasets within this conjugation product set.

3D Image Processing - Panel B

3D Volume Projection = Precise
Appearance = Threshold 2% all channels, Ramp 98% all channels, Maximum 100% all channels
Background = Black
Light = Brightness 100%, Azimuth 80°, Elongation -130°, Enabled Directional Lighting, Enabled Tone Mapping
Projection = View Angle 35°, Scale Z 100%, Reverse Z-Axis NOT Selected, Stereo Anaglyph NOT Selected, Camera Separation 5% (deselected), Parallax Shift 0% (deselected)

Clipping Image Processing - Panel B

Clipping planes are introduced in Panel B to highlight the Rabbit anti-Human Phospho- ATM (Serine 1981) Recombinant Monoclonal within the nuclear compartment by adjusting or cutting away portions of the image using a triple-wedge cut, removing parts of the image in the X-Y, X-Z, and Y-Z planes.

X-Y = Activate was selected, textured opaque was chosen, and a white outline of the clipped perimeter was shown; Clip Back was selected, and Clip Front was NOT selected.

Position of Clip = -38%
Clip X = 0°
Clip Z = 0°

X-Z = Activate was selected, textured opaque was chosen, and a green outline of the clipped perimeter was shown; Clip Back was selected, and Clip Front was NOT selected.

Position of Clip = 0%
Clip Y = 45°
Clip Z = 0°

Y-Z = Activate was selected, textured opaque was chosen, and a red outline of the clipped perimeter was shown; Clip Back was selected, and Clip Front was NOT selected.

Position of Clip = 0%
Clip Y = -45°
Clip Z = 0°

Summary

Panel A depicts Airyscan super-resolution fluorescence microscopy of Rabbit anti-Human ATM.p (Serine 1981) Recombinant Monoclonal - Identifyn® SRM Alexa Fluor™ 647, IgG - (BLR031P) acquired at z-plane 81 of 161 following DNA damage induction. The ATM.p signal is pseudocolored white to enhance visual contrast and facilitate assessment of fluorescence distribution, signal intensity, and ATM.p-associated foci formation throughout the nucleus. Strong nuclear-associated localization and discrete punctate foci were observed with minimal background interference, supporting preservation of signal integrity and robust fluorophore performance following direct conjugation. Signal distribution and staining characteristics remained consistent with the corresponding unconjugated stepdown dataset generated using Rabbit anti-Human ATM.p (Serine 1981) Recombinant Monoclonal, IgG - (BLR031P) (Cat ID# - PA-RR 000012), as well as the associated widefield and confocal data points within this conjugation product dataset, demonstrating equivalent localization behavior and preservation of imaging performance across multiple microscopy modalities. Importantly, the Airyscan and STORM data points in this dataset further validate the conjugation across both conventional and super-resolution fluorescence microscopy modalities.

Panel B presents a three-dimensional volume-view Airyscan reconstruction of the same dataset, showing ATM.p displayed in the default 647 pseudocolor (red) alongside DAPI nuclear counterstaining. An orthogonal wedge-cut representation of the X-Y, X-Z, and Y-Z planes is utilized to visualize fluorescence distribution throughout the volumetric dataset and further assess nuclear-associated ATM.p localization across axial depth. The dataset demonstrates strong volumetric signal retention, discrete ATM.p-associated foci formation, and clear nuclear enrichment throughout the sampled cellular volume. Collectively, the Airyscan dataset further supports the robustness of the direct conjugation, preservation of fluorophore efficiency, and compatibility of Rabbit anti-Human ATM.p (Serine 1981) Recombinant Monoclonal - Identifyn® SRM Alexa Fluor™ 647, IgG - (BLR031P) with super-resolution fluorescence microscopy workflows.

Image Correction

NONE

Image by J.K. Bennett
Image Analysis and Data Presentation by B.T. Bennett

SOURCE PROVENANCE

Catalog	DC-000074
Stage	Airyscan
Instrument	ZEISS LSM 980
Microscope configuration	Zeiss LSM 980 Confocal with NIR Detection, Axio Observer.Z1/7, using a Plan-Apochromat 63x/1.40 Oil DIC M27, was used with the following parameters for each dye:
Structured source metadata values	57
Metadata source	PRESERVED_SOURCE_METHOD_PDF_TEXT
Cell model	HeLa
Image SHA-256	91EB4E1ED158C1938DA3B6D16C6A0DBB1AA909103AC43EE8607A150117443C75
Method PDF SHA-256	460EB6A0D98C31B69D11CC185669EB9F4CD817D11958F284F56684B744A359FB

ORIGINAL IMAGE EVIDENCE / SINGLE-MOLECULE STORM

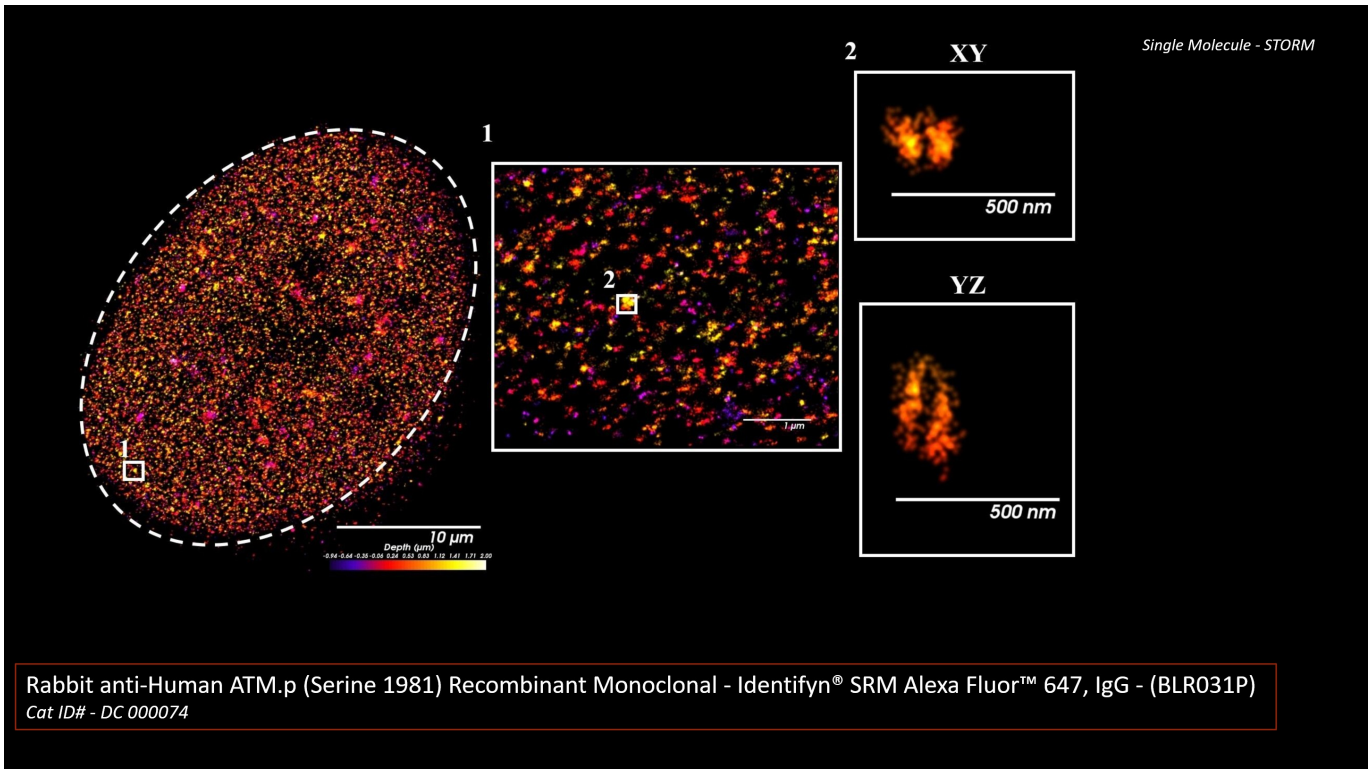

Rabbit anti-Human ATM.p (Serine 1981) Recombinant Monoclonal - Identifyn® SRM Alexa Fluor™ 647, IgG - (BLR031P)
Cat ID# - DC 000074

EVIDENCE TIER	Single-molecule STORM
INSTRUMENT	Bruker Vutara VXL
CELL MODEL	HeLa
DETECTED DYES	647
METADATA VALUES	79

STRUCTURED ACQUISITION METADATA / SINGLE-MOLECULE STORM

The values below were deterministically extracted from the preserved Identifyn method PDF text. They remain source-documented metadata, not new BENNETT measurements.

FIELD	SOURCE-DOCUMENTED VALUE
Platform / configuration	Bruker Vutara VXL Biplane Single Molecule Microscope, using an Olympus 60x/1.30 Silicon Oil Objective, was used with the following parameters:
Objective	Olympus 60x/1.30 Silicon Oil Objective
Number of Probes	1
Number of Simultaneous Probes	1
Number of Reference Probes	1
Camera	Both Cameras
Color Channel	Both Channels
Probe Capture Mode	Interleaved
Z -Stack Capture Mode	Interleaved
Multiple Location Capture	Not selected
Post Record Reference	Not Selected
Fluidics	Not Selected
Autofocus Drift Correction	On
Biplane Module	635 nm Dichroic
Objective	Silicon Selected
Stage Insert	Rectangular Selected
Coarse Focus Position	8-Well Chamber Selected
Dichroic	SuperRes
PSF	(Red, Orange)
Heater	Current: 26
Recording Vertical Field of View	100%
Widefield Camera Exposure Time	100 ms | 20 ms
Super Resolution Camera Exposure Time	20 ms
Widefield Camera Binning	1
Per-Probe Exposure Time	Selected
Predefined Probe	First probe: 640 nm (635 nm Dichroic); First reference probe: 640 nm (635 nm Dichroic)
Photoactivation/Imaging Laser	0% Selected
Exposure Time	20 ms Selected
Record Workflow	Selected Options
View Mode	Widefield 200 µm
Capture Mode	Live
Piezo Current	186.2 µm

FIELD	SOURCE-DOCUMENTED VALUE
Widefield 640nm	0.1X Neutral Density Filter: Selected, @ 0.2% Laser Input
Reference Probe 1 Laser control 640 nm (635 nm Dichroic)	Not Selected
Widefield camera Exposure Time	100 ms
Widefield Laser	"Widefield 640 nm" was deselected, and "calibrate" under Autofocus was selected.
Current Position	-0.979
Current Intensity	4.5
Calibration Value	-5070 nm/unit
Autofocus Mode	Pre-Capture
SuperRes	50 µm is selected
Piezo Record	Begin: 185; End: 186.2
SuperRes 640nm	0.1X Neutral Density Filter: Selected, @ 0.02% Laser Input
Record Workflow - Record Tab	Capture Parameters
Frames	Probe 1: 200
Z Positions	6
Cycles	25
Time Points	1
Pause Between Cycles	Not Selected
Automatic Photoactivation Laser Control	Not Selected
Laser Power	30
Cutout Width	16 px
Max Frame Accumulation	1 frame
Max Accumulation Offset	1 px
Fiducial at Max Accumulation	Not selected
Max Particles Per Frame	No Max
Background SLPE Removal	Not Selected
Cutout/Background Removal	Not Selected
Preview Cutout Positions	Selected
Probe1	BG threshold: 10
Sizing Mode	Radial precision
Particle size	4 nm
Color by	Depth
Color Table	Single
Opacity Mode	Depth; Opacity 1: 0.2
Front-to-back Attenuation	Not Selected
Method	Particle (direct)

FIELD	SOURCE-DOCUMENTED VALUE
Time Intervals	8 Intervals
Pixel Size	50 nm
Smoothing	8.00
Radial precision	35
Axial precision	70
Clustering Algorithm	DBSCAN
Maximum Particle Distance	0.1 um
Maximum Particle Count to Form Cluster	10
Compute Hulls	Not Selected
Compute Density Isosurfaces	Not Selected
Edit Settings	All Probes
Compute	Selected
Following Cluster Analysis Computation, under the Results Tab, ID Unassigned	Deselected

SOURCE METHOD

The text below is carried from the preserved Identifyn source record. Typography and pagination have been normalized for this preservation dossier; scientific wording has not been editorially rewritten.

Identifyn Standards for Optical Microscopy Methods™

Identifyn® Primary Antibody

Rabbit anti-Human ATM.p (Serine 1981) Recombinant Monoclonal, IgG - Identifyn® SRM Alexa Fluor™ 647 IgG - (BLR031P)
Cat ID# - DC 000074

ATM (ataxia-telangiectasia mutated) is a crucial serine/threonine kinase that plays a central role in the DNA damage response (DDR), particularly in response to DNA double-strand breaks (DSBs). ATM's activation and subsequent phosphorylation cascades are essential for detecting DNA damage and initiating repair processes. Here's a detailed overview of how ATM is activated, its targets, and its role in the DDR:

Activation of ATM
In response to DNA damage, particularly DSBs, ATM is activated through a series of events:

Detection of DNA Breaks: ATM can sense DNA breaks by associating with the MRN complex (MRE11, RAD50, and NBS1). This complex recognizes DSBs, leading to ATM's recruitment to the damaged site.

Autophosphorylation: Upon detection of DNA damage, ATM undergoes autophosphorylation at serine 1981 (S1981), leading to its activation. This phosphorylation event is critical for ATM's kinase activity and its ability to phosphorylate downstream targets.

Dimer-to-Monomer Transition: In its inactive form, ATM is a dimer. It transitions to an active monomeric state upon activation, allowing it to interact with and phosphorylate various downstream proteins.

Phosphorylation Targets of ATM

Once activated, ATM phosphorylates many proteins involved in the DNA damage response, cell cycle regulation, and apoptosis. Here are some critical targets of ATM:

CHK2: ATM phosphorylates CHK2, a cell cycle checkpoint control kinase. This phosphorylation helps to halt the cell cycle, allowing time for DNA repair.

p53: ATM phosphorylates p53, activating this tumor suppressor, leading to cell cycle arrest or apoptosis if the damage is irreparable.

H2AX: ATM phosphorylates histone H2AX, forming γ-H2AX, a marker of DNA damage. This modification helps signal the presence of DSBs and recruit DNA repair machinery.

BRCA1: ATM's phosphorylation of BRCA1 is critical for homologous recombination, a key DNA repair pathway for DSBs.

NBS1: As part of the MRN complex, NBS1 phosphorylation by ATM enhances the complex's DNA repair functions.

53BP1: ATM phosphorylation of 53BP1 helps recruit this protein to sites of DSBs, guiding repair pathways like non-homologous end joining (NHEJ).

Role of ATM Phosphorylation in DNA Repair

ATM-mediated phosphorylation plays a central role in coordinating the DNA damage response:

Signal Propagation: Phosphorylation cascades initiated by ATM amplify the signal for DNA damage, ensuring an efficient response.

Recruitment of Repair Machinery: Phosphorylation of specific proteins helps recruit DNA repair complexes to the sites of DNA damage.

Cell Cycle Regulation: ATM's activation can lead to cell cycle checkpoints, preventing cells from dividing with damaged DNA.

Apoptosis: If the DNA damage is too severe to repair, ATM's activation can lead to apoptosis, preventing the propagation of damaged cells

ATM's phosphorylation in response to DNA damage is crucial for detecting DNA double-strand breaks and coordinating the DNA damage response. By phosphorylating a range of critical proteins, ATM orchestrates a complex network of signaling events that facilitate DNA repair, cell cycle regulation, and apoptosis, thereby maintaining genomic stability.

Methods

HeLa cells were grown in a µ-Slide 8 Well high-Glass Bottom Ibidi chamber. DNA damage was induced via treatment with 2 µM Etoposide-spiked complete growth media for 12 hours, followed by -20 °C methanol fixation and blocked with Thermo Fisher Fish Serum Blocker (cat#37527X3). The primary antibody, Rabbit anti-Human ATM.p (Serine 1981) Recombinant Monoclonal - Identifyn® SRM Alexa Fluor™ 647, IgG - (BLR031P) was incubated for 1 hour at room temperature at a dilution of 1:100. Cells were washed 5 times in Identifyn®'s proprietary Wash Buffer followed by the addition of Identifyn®'s proprietary STORM Buffer to the sample chamber, enabling image acquisition.

Control Data - Primary Unconjugated Antibody

Microscope

Bruker Vutara VXL Biplane Single Molecule Microscope, using an Olympus 60x/1.30 Silicon Oil Objective, was used with the following parameters:

Calibration -

Calibration follows Identifyn®'s Calibration Standard Operating Procedure, which can be found here.

https://identifyn.com/storm-calibration

Image Acquisition -

SRX Software - Under the 'Single Molecule Localization' tab, 'Record' is selected and contains the following workflow tabs and parameters.

Configuration Tab - Capture Configuration

Number of Probes: 1
Number of Simultaneous Probes: 1
Number of Reference Probes: 1
Camera: Both Cameras
Color Channel: Both Channels
Probe Capture Mode: Interleaved
Z -Stack Capture Mode: Interleaved
Multiple Location Capture: Not selected
Post Record Reference: Not Selected
Fluidics: Not Selected
Autofocus Drift Correction: On

Microscope Configuration

Biplane Module: 635 nm Dichroic
Objective: Silicon Selected
Stage Insert: Rectangular Selected
Coarse Focus Position: 8-Well Chamber Selected
Dichroic: SuperRes
PSF: (Red, Orange)
Heater: Current: 26

Camera Configuration

Recording Vertical Field of View: 100%
Widefield Camera Exposure Time: 100 ms
Super Resolution Camera Exposure Time: 20 ms
Widefield Camera Binning: 1
Per-Probe Exposure Time: Selected

Probe Configuration

Predefined Probe: First probe: 640 nm (635 nm Dichroic); First reference probe: 640 nm (635 nm Dichroic)
Photoactivation/Imaging Laser: 0% Selected
Exposure Time: 20 ms Selected

Experiment Configuration

Record Workflow: Selected Options
View Mode: Widefield 200 µm
Capture Mode: Live

Stage and Piezo Selection

Examination of the Sample

Cell(s) or Cellular Structure Localization - The red-bordered box identifies the area of the SuperRes view and defines a suitable cell(s) or cellular structure. The cell(s) or structures are optimally focused.

Piezo Current: 186.2 µm

Probe 1 Laser control 640 nm (635 nm Dichroic)

Widefield 640nm: 0.1X Neutral Density Filter: Selected, @ 0.2% Laser Input
Reference Probe 1 Laser control 640 nm (635 nm Dichroic): Not Selected

Advanced Tools Option

Widefield camera Exposure Time: 100 ms
Default values are maintained unless otherwise noted.

Widefield Laser: "Widefield 640 nm" was deselected, and "calibrate" under Autofocus was selected.

Autofocus - Calibration Values

Current Position: -0.979
Current Intensity: 4.5
Calibration Value: -5070 nm/unit
Autofocus Mode: Pre-Capture

View Mode

SuperRes: 50 µm is selected

Capture Mode

Live

Stage and Piezo Selection

Cell(s) or Cellular Structure Localization - Positioning of the target cell or subsection is optimized and properly focused

Piezo Record: Begin: 185; End: 186.2

Probe 1 Laser control 640 nm (635 nm Dichroic)

SuperRes 640nm: 0.1X Neutral Density Filter: Selected, @ 0.02% Laser Input

Reference Probe 1 Laser control 640 nm (635 nm Dichroic)

Not Selected

Advanced Tools

Widefield Camera Exposure Time: 20 ms
Default values are maintained unless otherwise noted.

Record Workflow - Record Tab: Capture Parameters

Frames: Probe 1: 200
Z Positions: 6
Cycles: 25
Time Points: 1
Pause Between Cycles: Not Selected
Automatic Photoactivation Laser Control: Not Selected

Probe 1 Laser control 640 nm (635 nm Dichroic)

Laser Power: 30

Expert Configuration Options - The Localization Tab

Beyond the values shown, all other parameters were set to their default values.

Localization

Cutout Width: 16 px
Max Frame Accumulation: 1 frame
Max Accumulation Offset: 1 px
Fiducial at Max Accumulation: Not selected
Max Particles Per Frame: No Max
Background SLPE Removal: Not Selected
Cutout/Background Removal: Not Selected
Preview Cutout Positions: Selected

Record Workflow - Localization Tab

Data Collection

The folder is created automatically with the localization file for this image acquisition.

Recording Summary

All parameters were carried over from previous tabs and are kept except:

Probe1: BG threshold: 10

Region of Interest -

Not selected

Display -

Was deployed to inspect if the BG threshold applied chooses localizations in an expected manner

Record Workflow - View Tab

Region of Interest

Default values

Visualization Parameters

Point Splatting
Sizing Mode: Radial precision
Particle size: 4 nm
Color by: Depth
Color Table: Single
Opacity Mode: Depth; Opacity 1: 0.2
Front-to-back Attenuation: Not Selected

Post Acquisition analysis - View Tab

Drift Correction - Computed with the following parameters:

Method: Particle (direct)
Time Intervals: 8 Intervals
Pixel Size: 50 nm
Smoothing: 8.00

Advanced Particle Filters - Applied to the drift-corrected data with the following parameters

Radial precision: 35
Axial precision: 70

The other parameters were not applied.

Statistical Analysis - Computed to clean low background signals.

Statistics Dialog - Cluster Analysis

Clustering Algorithm: DBSCAN

Parameters

Maximum Particle Distance: 0.1 um
Maximum Particle Count to Form Cluster: 10
Compute Hulls: Not Selected
Compute Density Isosurfaces: Not Selected
Edit Settings: All Probes
Compute: Selected
Following Cluster Analysis Computation, under the Results Tab, ID Unassigned: Deselected

Summary

Collectively, the STORM dataset demonstrates that Rabbit anti-Human ATM.p (Serine 1981) Recombinant Monoclonal - Identifyn® SRM Alexa Fluor™ 647, IgG - (BLR031P) maintained strong fluorescence performance, localization fidelity, and nanoscale structural signal integrity under demanding single-molecule localization microscopy conditions. STORM imaging fundamentally relies on sufficient fluorophore brightness, stable photoswitching behavior, reproducible blinking kinetics, and resistance to photobleaching to generate accurate single-molecule localization events. These requirements often pose significant limitations for conventional direct conjugates in high-resolution localization workflows.

Importantly, the Identifyn® direct conjugate maintained robust signal intensity, stable localization performance, strong signal-to-noise characteristics, and reproducible ATM.p-associated nanoscale fluorescence organization throughout volumetric STORM acquisition, drift correction, advanced particle filtering, and DBSCAN cluster-analysis workflows. Despite extremely low SuperRes laser-input conditions, the direct conjugate preserved discrete ATM.p-associated fluorescence territories and biologically coherent structural organization highly consistent with the corresponding unconjugated Rabbit anti-Human ATM.p (Serine 1981) Recombinant Monoclonal, IgG - (PA-RR 000012) stepdown datasets generated across widefield, confocal, and Airyscan modalities.

Unlike many conventional direct conjugates that exhibit diminished photon output, unstable blink kinetics, elevated background fluorescence, localization artifacts, or fluorophore instability during prolonged single-molecule acquisition workflows, Rabbit anti-Human ATM.p (Serine 1981) Recombinant Monoclonal - Identifyn® SRM Alexa Fluor™ 647, IgG - (BLR031P) demonstrated compatibility with demanding super-resolution localization microscopy conditions while preserving biologically coherent ATM.p-associated structural organization. Collectively, these findings further support

the ability of the Identifyn® direct conjugation platform to maintain fluorophore efficiency, photoswitching compatibility, signal integrity, and localization fidelity under advanced STORM imaging workflows where conventional direct conjugates frequently fail.

Image by P. Raut
Image Analysis and Data Presentation by B.T. Bennett

SOURCE PROVENANCE

Catalog	DC-000074
Stage	Single-molecule STORM
Instrument	Bruker Vutara VXL
Microscope configuration	Bruker Vutara VXL Biplane Single Molecule Microscope, using an Olympus 60x/1.30 Silicon Oil Objective, was used with the following parameters:
Structured source metadata values	79
Metadata source	PRESERVED_SOURCE_METHOD_PDF_TEXT
Cell model	HeLa
Image SHA-256	7C9B143C02A779962C1981ABD6F71D89A13009641BEC8828E9E0309353244F37
Method PDF SHA-256	7DE94EA22B2FB78A9F111A1A2234E31DACA6BDB3F0E1938F61215B14B5BFEC59